Conditions and growth rate of Rayleigh instability in a Hall thruster under the effect of ion temperature

Hitendra K. Malik* and Sukhmander Singh

Plasma Waves and Particle Acceleration Laboratory, Department of Physics, Indian Institute of Technology Delhi, New Delhi 110 016, India

(Received 1 November 2010; revised manuscript received 16 January 2011; published 15 March 2011)

Rayleigh instability is investigated in a Hall thruster under the effect of finite temperature and density gradient of the plasma species. The instability occurs only when the frequency of the oscillations ω falls within a frequency band described by $k_y u_0 + \frac{1}{k_y}\frac{\partial^2 u_0}{\partial x^2} + \frac{\Omega}{k_y n_0}\frac{\partial n_0}{\partial x} \ll \omega < \sqrt{\frac{Y_i T_i k_y^2}{M} + \frac{\omega_{pi}^2(\Omega^2 + Y_e T_e k_y^2/m)}{(\omega_{pe}^2 + \Omega^2 + Y_e T_e k_y^2/m)}}$, where u_0 is the drift velocity of the electrons, Ω is their gyration frequency under the effect of the magnetic field, k_y is the wave propagation constant, n_0 is the plasma density together with $\partial n_0/\partial x$ as the density gradient, and $T_i(T_e)$, $M(m)$, $Y_i(Y_e)$, and $\omega_{pi}(\omega_{pe})$ are the temperature, mass, specific heat ratio, and plasma frequency of the ions (electrons), respectively. A relevant Rayleigh equation is derived and solved numerically using the fourth-order Runge-Kutta method for investigating the perturbed potential under the effect of electron drift velocity, channel length, magnetic field, ion temperature, and electron temperature. The instability grows faster because of the magnetic field, ion temperature, and drift velocity of the electrons but its growth rate is reduced because of the electron temperature, channel length, and also its far distances from the anode.

DOI: 10.1103/PhysRevE.83.036406 PACS number(s): 52.50.Dg, 52.75.Di, 52.25.Fi, 52.70.Kz

I. INTRODUCTION

A Hall thruster is one of the most efficient devices for space propulsion. This is an annular device in which a propellant, usually xenon, is ionized and then accelerated by electrostatic force (corresponding field $\vec{E}$) to create propulsive thrust. The thrust is generated by ion acceleration in a quasineutral plasma. A Hall thruster has a virtual cathode which is located near the zone where the magnetic field $\vec{B}$ is maximum. In this zone the axial electron mobility is reduced as the electrons are trapped on the Larmor orbits. Moreover, the ratio E/B is selected such that the electron gyroradius is much smaller but the ion gyroradius is much larger than the anode to cathode spacing. Hence, the ions can be freely accelerated out of the device. Upon exiting the device the ion beam is neutralized by the electrons generated from the virtual cathode, thus maintaining quasineutrality within the plasma plume.

Hall thrusters are more suitable for a long-term mission in space than other electric thrusters [1–6]. However, in such thrusters, due to the difference in the drift velocities of the electrons and ions and their charge difference, an electric field is produced in the azimuthal direction. On the production of this electric field the electrostatic waves are generated in the azimuthal direction. In the presence of a density gradient these waves can gain free energy from the density gradient, grow up, and finally become unstable. In addition, the instabilities of the discharge current and plasma oscillations can occur in these devices which play an important role in controlling the transport, conduction, and mobility. Hence, in order to improve the performance of the Hall thrusters, we need to better understand inner physical phenomena related to waves and instabilities. In this direction Choueiri [6] has discussed different types of discharge instabilities in Hall thrusters ranging from kilo-Hertz to giga-Hertz domain. Chable and Rogier [7] have numerically studied Buneman's instability in a Hall thruster and examined the role played by coupling between the electric field and the ion current. Barral and Peradzynski [8] have studied low frequency oscillations under the effect of ionization in a Hall thruster. Keidar [9] has modeled plasma dynamics and ionization of the propellant gas within the anode holes used for gas injection of a Hall thruster. Meezan *et al.* [10] have presented an analysis for the anomalous electron mobility in a coaxial Hall discharge plasma. Thomas *et al.* [11] have developed a diagnostic for the azimuthal drift current in a coaxial $\vec{E} \times \vec{B}$ discharge plasma. A high-frequency (HF) instability in the range of 5–10 MHz has also been reported experimentally by Litvak *et al.* [12]. Lazurenko *et al.* [13] have experimentally studied the high-frequency instability and anomalous electron transport phenomena in a Hall thruster. Litvak and Fisch [14] have analytically studied gradient-driven Rayleigh-type instabilities in Hall plasma thrusters by neglecting the thermal motions of the plasma species. Ducrocq *et al.* [15] have investigated high-frequency electron drift instability in the cross-field configuration of a Hall thruster together with the effect of distorted electron distribution functions obtained in particle-in-cell simulations. Barral and Ahedo [16] have developed a low-frequency model of breathing oscillations in Hall discharges where they observed that unstable modes are strongly nonlinear and are characterized by frequencies obeying a scaling law different from that of linear modes.

For the sake of simplicity the temperature of plasma species in most of the studies has been neglected, although it significantly affects the efficiency and performance of the thrusters via thermal motions of the ions and electrons [17,18]. Therefore, in order to realize the exact behavior and the consequences of finite temperatures, it is very important to investigate the instabilities in Hall thrusters by including the

*hkmalik@physics.iitd.ac.in; hkmalik@hotmail.com

finite temperatures of the plasma species. Hence, in the present article we have analytically derived the conditions and growth rate of Rayleigh instability in a Hall thruster using relevant equations along with the contribution of the pressure gradient term. For this realistic situation an azimuthally propagating mode becomes unstable when its oscillation frequency falls within a frequency band that shows a dependence on the plasma parameters, drift velocity of the electrons, azimuthal wave number, and magnetic field.

II. THEORETICAL MODEL

We consider a Hall thruster with a two-component plasma consisting of ions and electrons immersed in a magnetic field $\vec{B} = B_0\hat{z}$ such that the electrons are magnetized and the ions are unmagnetized. The applied perturbations are assumed to be potential and nondissipative and the ionization processes are not taken into account. With regard to the geometry, the x axis is taken along of the axis of the thruster (i.e., along the applied electric field $\vec{E}$) and the z axis is taken along the radius of the thruster radius along which the magnetic field $\vec{B}$ is applied. Hence, the y axis corresponds to the azimuthal dimension. Under this situation we write the basic fluid equations for the ion and electron fluids as

$$\frac{\partial n_i}{\partial t} + \vec{\nabla}\cdot(\vec{\upsilon}_i n_i) = 0, \tag{1}$$

$$Mn_i\left[\frac{\partial \vec{\upsilon}_i}{\partial t} + (\vec{\upsilon}_i\cdot\vec{\nabla})\vec{\upsilon}_i\right] = en_i\vec{E} - \vec{\nabla}p_i, \tag{2}$$

$$\frac{\partial n_e}{\partial t} + \vec{\nabla}\cdot(\vec{\upsilon}_e n_e) = 0, \tag{3}$$

$$mn_e\left[\frac{\partial \vec{\upsilon}_e}{\partial t} + (\vec{\upsilon}_e\cdot\vec{\nabla})\vec{\upsilon}_e\right] = -n_e e\vec{E} - n_e e(\vec{\upsilon}_e\times\vec{B}) - \vec{\nabla}p_e - n_e m\nu_e\vec{\upsilon}_e. \tag{4}$$

In the above equations n_i is the ion density, $M$is the ion mass, $\vec{\upsilon}_i$ is the ion fluid velocity, $\vec{E}$ is the axial electric field, n_e is the electron density, m is the electron mass, $\vec{\upsilon}_e$ is the electron fluid velocity, and ν_e is the collision momentum transfer frequency between the electrons and neutral atoms.

We use the linearized form of the above equations for small perturbations of ion and electron densities, their velocities, and electric field. We represent perturbed densities by n_i and n_e, velocities by $\vec{\upsilon}_i$ and $\vec{\upsilon}_e$ where their unperturbed values are taken as υ_0 and u_0, respectively, together with υ_0 as the ions' initial drift in the x direction and u_0 as the electrons' drift in the y direction. The unperturbed density is taken as n_0 and the perturbed value of the electric field is taken as $\vec{E}$ (corresponding potential ϕ). Hence, the linearized form of Eqs. (1)–(4) reads

$$\frac{\partial n_i}{\partial t} + \upsilon_0\frac{\partial n_0}{\partial x} + \upsilon_x\frac{\partial n_0}{\partial x} + \upsilon_0\frac{\partial n_i}{\partial x} + n_0(\vec{\nabla}\cdot\vec{\upsilon}_i) = 0, \tag{5}$$

$$\frac{\partial \vec{\upsilon}_i}{\partial t} + \upsilon_0\frac{\partial \vec{\upsilon}_i}{\partial x} = \frac{e}{M}\vec{E} - \frac{\vec{\nabla}p_i}{n_0 M}, \tag{6}$$

$$\frac{\partial n_e}{\partial t} + u_0\frac{\partial n_e}{\partial y} + n_0(\vec{\nabla}\cdot\vec{\upsilon}_e) + \upsilon_{ex}\frac{\partial n_0}{\partial x} = 0, \tag{7}$$

$$\frac{\partial \vec{\upsilon}_e}{\partial t} + u_0\frac{\partial \vec{\upsilon}_e}{\partial y} = -\frac{e}{m}(\vec{E} + \vec{\upsilon}_e\times\vec{B}_0) - \frac{\vec{\nabla}p_e}{mn_0} - \nu_e\vec{\upsilon}_e. \tag{8}$$

We seek the solutions of the above equations for which we have $A = A\exp(i\omega t - ik_y y)$ for the oscillating quantities, that is, densities n_i, n_e, velocities $\vec{\upsilon}_i$, $\vec{\upsilon}_e$, and electric field $\vec{E}$. Here ω is the frequency of oscillations and k_y is the propagation constant. For the ion motion we use the assumption that the frequency of the perturbations we consider is high enough in comparison with the ion flow velocity, that is, $\upsilon_i \ll \omega L$ together with L as the inhomogeneity length along the channel. With the help of Eqs. (5) and (6) we obtain the following expression for the perturbed ion density in terms of the perturbed electric potential ϕ:

$$n_i = \frac{en_0}{\left(M\omega^2 - Y_i T_i k_y^2\right)}\left(k_y^2\phi - \frac{\partial^2\phi}{\partial x^2} - \frac{Y_i T_i}{en_0}\frac{\partial^2 n_0}{\partial x^2}\right). \tag{9}$$

On the other hand, we obtain from Eq. (8)

$$(\omega - k_y u_0 - i\nu_e)\upsilon_x = \frac{e}{m}\frac{\partial\phi}{\partial x} - \Omega\upsilon_y - \frac{Y_e T_e}{mn_0}\frac{\partial n_0}{\partial x}, \tag{10}$$

$$(\omega - k_y u_0 - i\nu_e)\upsilon_y + \upsilon_x\frac{\partial u_0}{\partial x} = -ik_y\frac{e}{m}\phi + \Omega\upsilon_x + \frac{ik_y n_e Y_e T_e}{n_0 m}. \tag{11}$$

Here, $\Omega = \frac{eB_0}{m}$ is taken as the electron gyrofrequency and $u_0 = -\frac{E_0}{B_0}$ as the initial drift of the electrons in the y direction. The previous equations are solved for the x and y components of the electron velocities for which we obtain

$$\upsilon_x = \frac{\frac{e}{m}i\hat{\omega}\frac{\partial\phi}{\partial x} + \frac{e}{m}ik_y\Omega\phi - \frac{ik_y Y_e T_e\Omega n_e}{mn_0} - \frac{Y_e T_e i\hat{\omega}}{mn_0}\frac{\partial n_0}{\partial x}}{\Omega^2 - \hat{\omega}^2 - \Omega\frac{\partial u_0}{\partial x}}, \tag{12}$$

$$\upsilon_y = \frac{e}{m\Omega}\frac{\partial\phi}{\partial x} - \frac{Y_e T_e}{mn_0\Omega}\frac{\partial n_0}{\partial x} + \frac{\frac{e}{m}\hat{\omega}^2\frac{\partial\phi}{\partial x} + \frac{e}{m}\hat{\omega}k_y\Omega\phi - \frac{\hat{\omega}k_y Y_e T_e\Omega n_e e}{mn_0} - \frac{\hat{\omega}^2 Y_e T_e}{mn_0}\frac{\partial n_0}{\partial x}}{\left(\Omega^2 - \hat{\omega}^2 - \Omega\frac{\partial u_0}{\partial x}\right)\Omega}, \tag{13}$$

together with

$$\hat{\omega} = \omega - k_y u_0 - i\nu_e. \tag{14}$$

Furthermore, with the assumption $\Omega \gg \omega, k_y u_0, \frac{\partial u_0}{\partial x}$ and ν_e, the components υ_x and υ_y take the form

$$\upsilon_x = \frac{e}{\Omega^2 m}\left(i\hat{\omega}\frac{\partial\phi}{\partial x} + i\Omega k_y\phi + \frac{\partial u_0}{\partial x}ik_y\phi - \frac{i\Omega n_e k_y Y_e T_e}{en_o} - \frac{Y_e T_e i\hat{\omega}}{en_0}\frac{\partial n_0}{\partial x} - \frac{ik_y n_e Y_e T_e}{en_0}\frac{\partial u_0}{\partial x}\right), \tag{15}$$

$$\upsilon_y = \frac{e}{\Omega m}\left(\frac{\partial\phi}{\partial x} + \frac{k_y\hat{\omega}\phi}{\Omega} + \frac{k_y\hat{\omega}\phi}{\Omega^2}\frac{\partial u_0}{\partial x} - \frac{\hat{\omega}n_e k_y Y_e T_e}{e\Omega n_0} - \frac{Y_e T_e}{en_0}\frac{\partial n_0}{\partial x} - \frac{\hat{\omega}^2 n_e k_y Y_e T_e}{\Omega^2 n_o}\frac{\partial u_0}{\partial x}\right). \tag{16}$$

Along with the above equations we solve the electron continuity equation (7) and obtain the perturbed electron density n_e as

$$n_e = \frac{\frac{en_0}{m\Omega^2}\left[\left(k_y^2\phi - \frac{\partial^2\phi}{\partial x^2}\right)\left(1 - \frac{i\nu_e}{\omega - k_y u_0}\right) + \frac{k_y}{\omega - k_y u_0}\left(\Omega\frac{\partial}{\partial x}\ln\frac{B_0}{n_0} - \frac{\partial^2 u_0}{\partial x^2}\right)\phi\right] - \frac{Y_e T_e}{(\omega - k_y u_0)m\Omega}\left(k_y\frac{\partial n_0}{\partial x} - \frac{\hat{\omega}}{\Omega}\frac{\partial^2 n_0}{\partial x^2}\right)}{1 - \frac{Y_e T_e k_y}{(\omega - k_y u_0)m\Omega^2}\left(\frac{\partial^2 u_0}{\partial x^2} + \Omega\frac{\partial n_0}{n_0\partial x} - \hat{\omega}k_y\right)}. \tag{17}$$

Finally, we use the expressions for the perturbed ion density n_i and electron density n_e in the Poisson's equation $\varepsilon_0\nabla^2\phi = e(n_e - n_i)$ in order to obtain

$$\left(\frac{\partial^2\phi}{\partial x^2} - k_y^2\phi\right)\left[1 + \frac{\omega_{pe}^2/\Omega^2}{1 - \frac{Y_e T_e k_y}{(\omega - k_y u_0)m\Omega^2}\left(\frac{\partial^2 u_0}{\partial x^2} + \Omega\frac{\partial n_0}{n_0\partial x} - \hat{\omega}k_y\right)} - \frac{e^2 n_0}{\left(M\omega^2 - Y_i T_i k_y^2\right)\varepsilon_0}\right]$$
$$- \frac{\frac{\omega_{pe}^2}{\Omega^2}\frac{k_y\varphi}{(\omega - k_y u_0)}\left(\Omega\frac{\partial}{\partial x}\ln\frac{B_0}{n_0} - \frac{\partial^2 u_0}{\partial x^2}\right)}{1 - \frac{Y_e T_e k_y}{(\omega - k_y u_0)m\Omega^2}\left(\frac{\partial^2 u_0}{\partial x^2} + \Omega\frac{\partial n_0}{n_0\partial x} - \hat{\omega}k_y\right)} - \frac{\frac{eY_e T_e}{(\omega - k_y u_0)\varepsilon_0 m\Omega}\left(k_y\frac{\partial n_0}{\partial x} - \frac{\hat{\omega}}{\Omega}\frac{\partial^2 n_0}{\partial x^2}\right)}{1 - \frac{Y_e T_e k_y}{(\omega - k_y u_0)m\Omega^2}\left(\frac{\partial^2 u_0}{\partial x^2} + \Omega\frac{\partial n_0}{n_0\partial x} - \hat{\omega}k_y\right)} - \frac{eY_i T_i}{\left(\frac{M\omega^2}{-Y_i T_i k_y^2}\right)\varepsilon_0}\frac{\partial^2 n_0}{\partial x^2} = 0, \tag{18}$$

where we have defined $\omega_{pi} = \sqrt{\frac{n_0 e^2}{M\varepsilon_0}}$ and $\omega_{pe} = \sqrt{\frac{n_0 e^2}{m\varepsilon_0}}$. This equation encompasses the terms of perturbed and unperturbed quantities. Since the first-order (perturbed) quantities cannot be explicitly expressed in term of zeroth-order (unperturbed) quantities we treat them separately by equating them to zero.

A. Calculation of growth rate of instability

In view of plasma generation in the thruster channel and neutralization of the ions at the exit of the thruster, it is obvious that the plasma density would attain maximum value in the middle of the channel. Hence, we assume the density and velocity distribution in the acceleration channel as

$$A_0 = A_{0\max}\left[\sin^2\left(\frac{\pi x}{d}\right) - \frac{1}{2}\right] \tag{19}$$

together with $A_{0\max}$ as the peak value of n_0 or u_0. Though in the real thruster the drift velocity distribution may be different, it simplifies the analytical calculations. In the above expressions for the density and drift velocity the coordinate x lies in the interval $0 < x < d$, where d is the channel length. We further simplify our calculations by neglecting the collisions ($\nu_e = 0$). The neglect of electron collisions with neutrals is justified for the present case of Rayleigh instability, which is developed by the density gradient and the magnetic field. Since in the presence of magnetic field the electron motion is confined, it is quite plausible that the collisions will have less consequence on the excitation of waves and instabilities.

Now for obtaining the growth rate of the instabilities we solve the unperturbed part of Eq. (18) with the expressions of n_0 and u_0 given by Eq. (19). After making mathematical simplifications we obtain the following dispersion equation:

$$\omega^3 - \omega^2 k_y\left(u_0 + \frac{\Omega d}{\pi}\tan(\xi)\right) + \frac{Y_i T_i}{M}\left(k_y^2 + \frac{2m\Omega^2}{Y_e T_e}\right)\omega$$
$$- \frac{2k_y Y_i T_i}{M}\left[\frac{u_0\Omega^2 m}{Y_e T_e} + \frac{u_0 k_y^2}{2} - \frac{2\Omega\pi}{d}\tan(\xi)\right.$$
$$\left. + 2u_0\left(\frac{\pi}{d}\right)^2\cos(\xi) - \frac{\Omega d k_y^2}{2\pi}\tan(\xi)\right] = 0 \tag{20}$$

together with $\xi = \frac{2\pi x}{d}$. The above equation is cubic in ω and has the following three roots:

$$\omega_1 = -\frac{1}{3}\left(a_1 + \sqrt[3]{\frac{m_1 + \sqrt{n}}{2}} + \sqrt[3]{\frac{m_1 - \sqrt{n}}{2}}\right), \tag{21}$$

$$\omega_2 = -\frac{1}{3}\left[a_1 - \left(\frac{1 + i\sqrt{3}}{2}\right)\sqrt[3]{\frac{m_1 + \sqrt{n}}{2}}\right.$$
$$\left. + \left(\frac{-1 + i\sqrt{3}}{2}\right)\sqrt[3]{\frac{m_1 - \sqrt{n}}{2}}\right], \tag{22}$$

$$\omega_3 = -\frac{1}{3}\left[a_1 - \left(\frac{1 - i\sqrt{3}}{2}\right)\sqrt[3]{\frac{m_1 + \sqrt{n}}{2}}\right.$$
$$\left. + \left(\frac{-1 - i\sqrt{3}}{2}\right)\sqrt[3]{\frac{m_1 - \sqrt{n}}{2}}\right]. \tag{23}$$

In the above expressions $m_1 = 2a_1^3 - 9a_1 a_2 + 27a_3$ and $n = m_1^2 - 4K^3$ together with $K = a_1^2 - 3a_2$. Also, a_1 and a_2 are the coefficients of ω^2 and ω terms in Eq. (20) and a_3 is the constant term, that is,

$$a_1 = k_y\left(u_0 + \frac{\Omega d}{\pi}\tan(\xi)\right), \quad a_2 = \frac{Y_i T_i}{M}\left(k_y^2 + \frac{2m\Omega^2}{Y_e T_e}\right),$$

and

$$a_3 = -\frac{2k_y Y_i T_i}{M}\left[\frac{u_0\Omega^2 m}{Y_e T_e} + \frac{u_0 k_y^2}{2} - \frac{2\Omega\pi}{d}\tan(\xi)\right.$$
$$\left. + 2u_0\left(\frac{\pi}{d}\right)^2\cos(\xi) - \frac{\Omega d k_y^2}{2\pi}\tan(\xi)\right].$$

Here it turns out that the root ω_1 is real but the roots ω_2 and ω_3 are complex. Moreover, it is seen that the root ω_3 corresponds to a growing mode or the instability if the below

mentioned condition is satisfied:

$$k_y^2 u_0^2 + \frac{4k_y^4 u_0 \Omega Y_e T_e M d^3 \tan^3 \xi}{27 Y_i T_i m \pi^3} + \frac{4 Y_i T_i m \Omega^2}{27 Y_e T_e M} > \frac{1}{27}\left(\frac{k_y \Omega d \tan \xi}{\pi}\right)^2 + \frac{2k_y^2 u_0 \Omega d \tan \xi}{3}. \tag{24}$$

B. Condition for Rayleigh instability

Now we examine the perturbed part of Eq. (18). This equation takes the following form when we use expression (23):

$$\frac{\partial^2 \phi}{\partial x^2} - k_y^2 \phi - \frac{\frac{\omega_{pe}^2}{\Omega^2}\frac{k_y \phi}{(\omega - k_y u_0)}\left(\Omega \frac{\partial}{\partial x} \ln \frac{B_0}{n_0} - \frac{\partial^2 u_0}{\partial x^2}\right)}{\left[1 - \frac{Y_e T_e k_y}{m\Omega^2}\left(\frac{\frac{\partial^2 u_0}{\partial x^2} + \Omega \frac{\partial n_0}{n_0 \partial x}}{(\omega - k_y u_0)} - k_y\right)\right]\left[1 - \frac{\omega_{pi}^2}{\omega^2\left(1 - \frac{Y_i T_i k_y^2}{M\omega^2}\right)}\right] + \frac{\omega_{pe}^2}{\Omega^2}} = 0. \tag{25}$$

It is interesting to note that this equation reduces to Eq. (25) of Litvak and Fisch [14] when the ion and electron temperatures are omitted. Moreover, the term $\frac{\omega_{pi}^2}{\omega^2}$ was neglected in Ref. [14] for the sake of simplicity. However, we retain all the terms arising due to the finite temperature of the plasma species and ion plasma frequency. Under this more realistic situation we obtain Eq. (25) which is a modified form of the well-known Rayleigh equation of fluid dynamics. This equation attains the identical form of the Rayleigh equation [19] if the following condition is met:

$$\omega \gg k_y u_0 + \frac{1}{k_y}\frac{\partial^2 u_0}{\partial x^2} + \frac{\Omega}{k_y n_0}\frac{\partial n_0}{\partial x}. \tag{26}$$

In addition, the oscillation frequency ω should satisfy the following condition:

$$\omega < \sqrt{\frac{Y_i T_i k_y^2}{M} + \frac{\omega_{pi}^2\left(\Omega^2 + Y_e T_e k_y^2/m\right)}{\left(\omega_{pe}^2 + \Omega^2 + Y_e T_e k_y^2/m\right)}}. \tag{27}$$

Based on Eqs. (26) and (27), it is inferred that the oscillations will grow into the Rayleigh instability only when their frequency remains within a frequency band described by the following inequalities:

$$k_y u_0 + \frac{1}{k_y}\frac{\partial^2 u_0}{\partial x^2} + \frac{\Omega}{k_y n_0}\frac{\partial n_0}{\partial x} \ll \omega < \sqrt{\frac{Y_i T_i k_y^2}{M} + \frac{\omega_{pi}^2\left(\Omega^2 + Y_e T_e k_y^2/m\right)}{\left(\omega_{pe}^2 + \Omega^2 + Y_e T_e k_y^2/m\right)}}. \tag{28}$$

It is evident that this frequency band is the consequence of the finite temperatures of the plasma species and the higher cutoff frequency attains larger values for the higher temperature of the ions and electrons. Hence, a broader frequency band is realized in a more realistic situation where the plasma species carry finite temperature. This interesting frequency band was not explored by other investigators [6–8,12–16,23,25] and is the new result. Based on this, the oscillations (perturbations) of only higher frequency would grow into instability if the plasma contains stronger density gradient, the electrons drift with higher velocity, or stronger magnetic field is applied. Moreover, the oscillations of larger wavelength or smaller k_y are found to be unstable even at lower frequency.

III. RESULTS OF GROWTH RATE AND PERTURBED POTENTIAL

In this section we plot various figures for investigating the variation of growth rate of the instability with magnetic field B_0, initial drift of the electrons u_0, channel length d, ion temperature T_i, and axial distance x. Moreover, Eq. (25) is solved numerically using a fourth-order Runge-Kutta method for the perturbed potential ϕ along with the use of boundary conditions $\phi(0) = \phi(d) = 0$, where d is the distance between the anode and cathode (channel length).

Figure 1 shows the variation of growth rate γ [$\equiv (\omega_3/\omega_{pi})$] of the instability with magnetic field when $T_e = 10$ eV, $T_i = 1$ eV, $Y_e = 2$, $Y_i = 2$, $n_0 = 10^{18}/\mathrm{m}^3$, $u_0 = 10^6$m/s, $k_y = 25/\mathrm{m}$, and $d = 5.5$ cm. These parameters are within the prescribed range as used in the literature [12,20–22] and realized in the experiment [22]. It is seen from the figure that the instability grows faster in the presence of stronger magnetic field. Wei *et al.* [23] also observed experimentally an enhancement in the growth rate of coupling instability with the magnetic field. The large growth rate is attributed

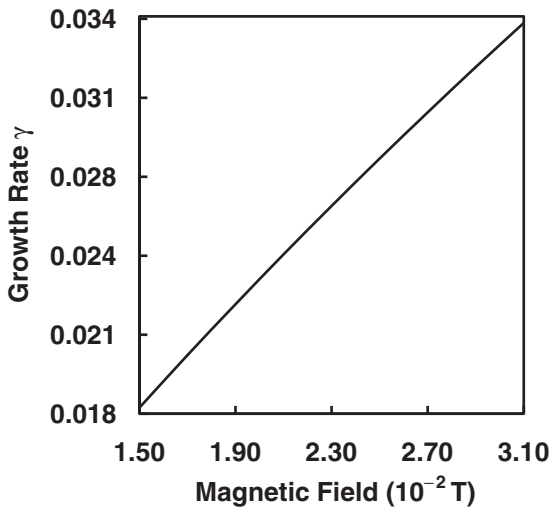

FIG. 1. Variation of growth rate γ with magnetic field in a plasma having X_e ions (mass = 131 amu), when $T_e = 10$ eV, $T_i = 1$ eV, $Y_e = 2$, $Y_i = 2$, $n_0 = 10^{18}/\mathrm{m}^3$, $u_0 = 10^6$ m/s, $k_y = 25/\mathrm{m}$, and $d = 5.5$ cm.

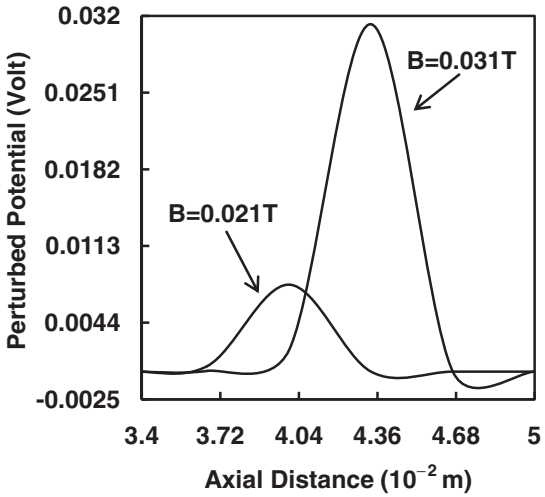

FIG. 2. Effect of magnetic field on the perturbed potential ϕ for the same parameters as in Fig. 1.

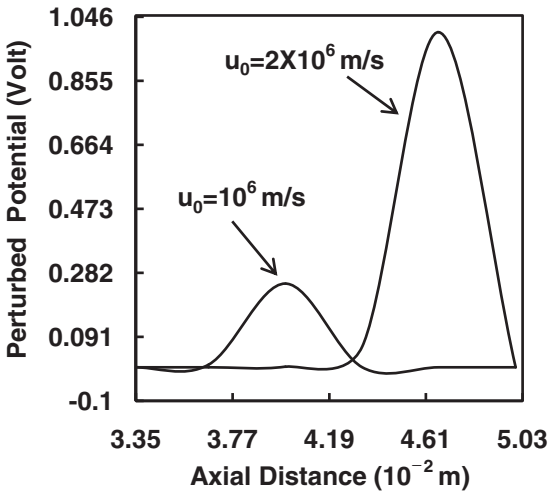

FIG. 4. Dependence of perturbed potential ϕ on the drift velocity of the electrons corresponding to Fig. 3.

to the nonuniformity of the velocity in the presence of a larger magnetic field. This can be understood based on Eq. (25) along with the condition (28) which describes the stability of ideal fluid flow with the lateral flow velocity nonuniformity. Since the presence of at least one point of inflection in the velocity profile is required for the Rayleigh instability, it is plausible that the nonuniformity in the velocity is enhanced in the presence of the magnetic field due to the electrons' gyratory motion and that the instability grows at a faster rate. Moreover, the presence of the magnetic field confines the electrons' trajectories and increases their residence time in the channel. This will enhance the oscillation frequency, resulting in a more unstable situation and hence the increased growth rate.

The perturbed potential distribution for the two different values of magnetic field is shown in Fig. 2, where it is seen that the potential increases with the increasing magnetic field. Similar results were reported by Keidar and Boyd [24] for the potential of plasma plume. The enhancement in perturbed potential with the magnetic field can be understood in the following manner. In the present case plasma jet enters a transverse magnetic field with a high supersonic directed velocity under the condition that the magnetic field is relatively weak so that only the electrons are magnetized, whereas the ions move out of the effect of magnetic field. However, ambipolar current less plasma flow across the magnetic field may require an electric field to appear under the above conditions. Therefore, we can expect the potential to increase across the magnetic field. This result is consistent with the behavior of growth rate of the instability (Fig. 1) with the magnetic field, where the instability grows faster.

In Fig. 3 we show the behavior of growth rate of the instability with initial drift velocity of the electrons. It is seen that the growth rate is increased for the larger drift velocity of the electrons. Since the drift velocity can be correlated with the discharge voltage, it can be said that the growth rate is increased with the discharge voltage. Esipchuk and Tilinin [25] also reported the proportionality of the frequency of drift instability to the discharge voltage. The cause of the

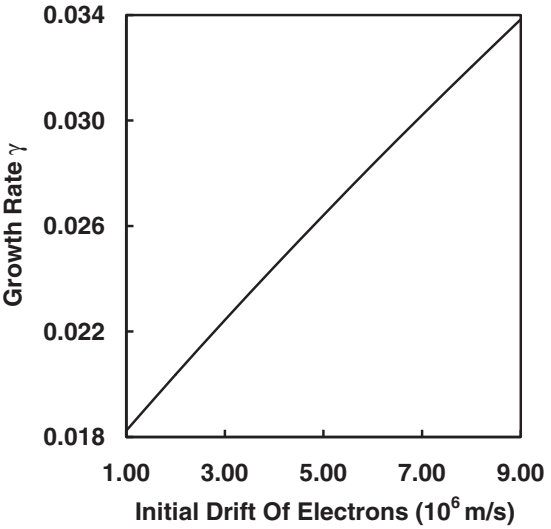

FIG. 3. Dependence of growth rate γ on the initial drift velocity u_0 of the electrons when $B_0 = 0.015$ T and other parameter are the same as in Fig. 1.

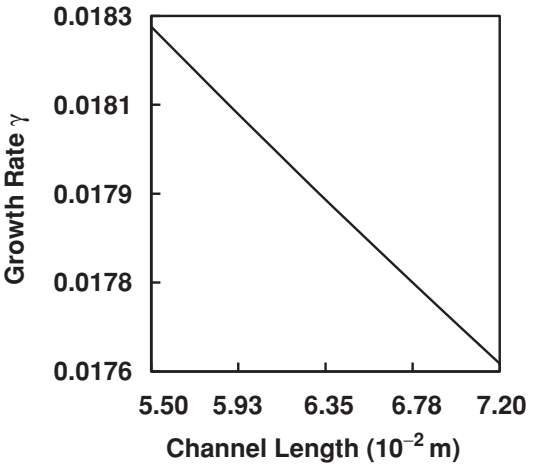

FIG. 5. Weak dependence of growth rate γ on the channel length when $B_0 = 0.015$ T and other parameter are the same as in Fig. 1.

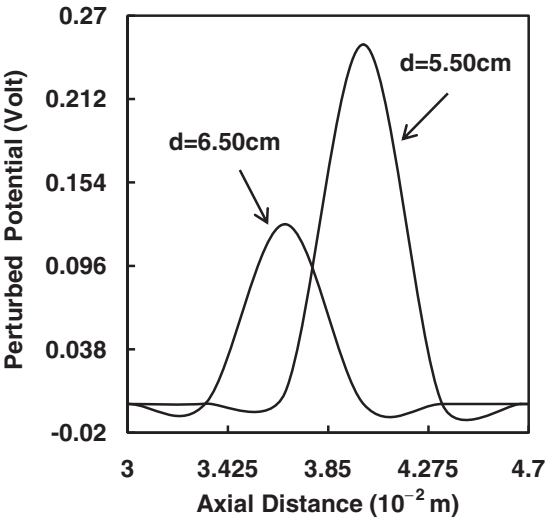

FIG. 6. Dependence of perturbed potential ϕ on the channel length d corresponding to Fig. 5.

increase in growth rate can also be understood as the strong coupling between the electric field and the electron current [7]. When we focus on the variation of the perturbed potential ϕ with the drift velocity in Fig. 4, we notice that the effect of drift velocity on the potential is in accordance with the variation of the growth rate. Similar behavior of the potential was reported experimentally by King *et al.* [26] for the potential of plasma plume.

In Fig. 5 we show the dependence of growth rate on the channel length. Clearly the growth rate of the instability decreases as we increase the channel length. This is obvious because the channel length can be viewed as the scale length of the plasma density gradient. For the larger channel length the density gradient becomes weaker due to the longer scale length, which results in more stability of the system or the reduction in the growth of the instability. Also, the corresponding perturbed potential goes down (as shown in Fig. 6).

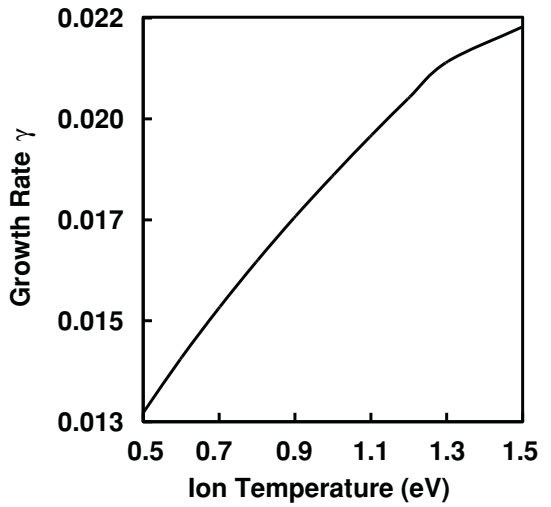

FIG. 7. Effect of ion temperature on the growth rate γ of the instability when $B_0 = 0.015$ T and other parameter are the same as in Fig. 1.

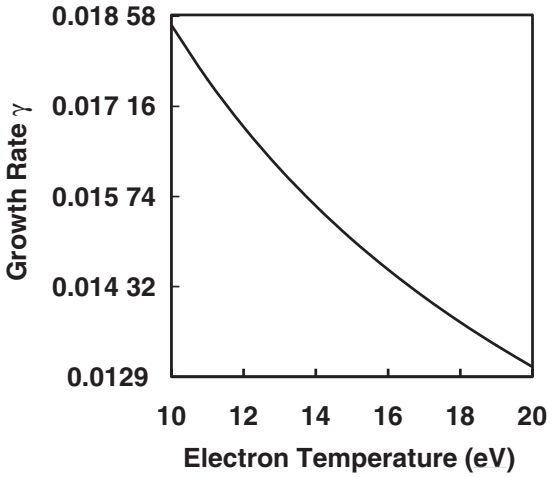

FIG. 8. Variation of growth rate γ with the electron temperature when $B_0 = 0.015$ T and other parameter are the same as in Fig. 1.

The reduction in the density gradient with an enhancement in the channel length can be explained based on Eq. (19), which shows that the density gradient $\frac{\partial n_0}{\partial x} = \frac{n_0 \pi}{d} \sin\left(\frac{2\pi x}{d}\right)$ and hence the density gradient scale length $\frac{n_0}{\partial n_0/\partial x} = \frac{d}{\pi} \operatorname{cosec}(\frac{2\pi x}{d})$. It is clear that with the increase of channel length d the effective density gradient gets reduced due to the enhanced scale length.

The effect of ion temperature on the growth rate of the instability is shown in Fig. 7, where we observe an enhancement in the growth rate with the ion temperature. This is attributed to the increased pressure gradient force. Since the increased pressure gradient force in the presence of higher ion temperature would have the same consequences as the stronger density gradient, it is obvious that the Rayleigh instability grows faster when the ions carry higher temperature. On the other hand, the electron temperature has opposite effect on the growth of the instability (Fig. 8). This is due to the reduced restoring force in the presence of higher thermal motion of the electrons. Under this situation lower frequency of oscillations is realized for the fixed wavelength and hence the reduced growth rate. The opposite effect of ion and electron temperatures on the growth rate can be understood based on

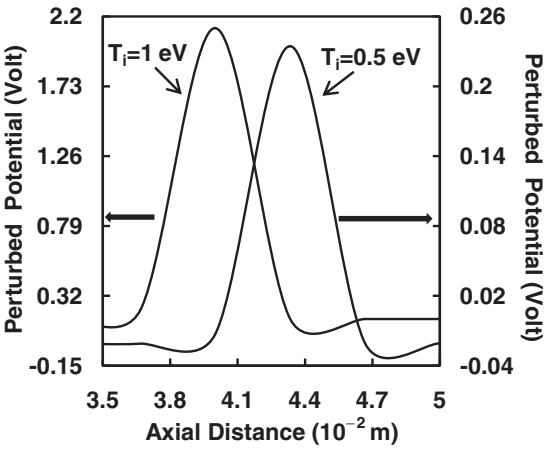

FIG. 9. Variation of perturbed potential ϕ with the ion temperature corresponding to Fig. 7.

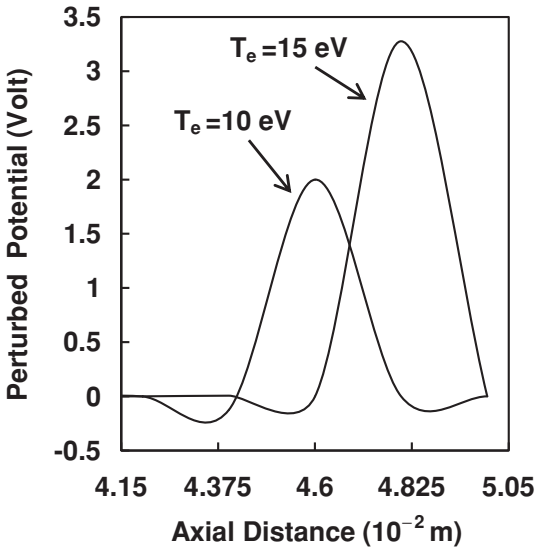

FIG. 10. Variation of perturbed potential ϕ with the electron temperature corresponding to Fig. 8.

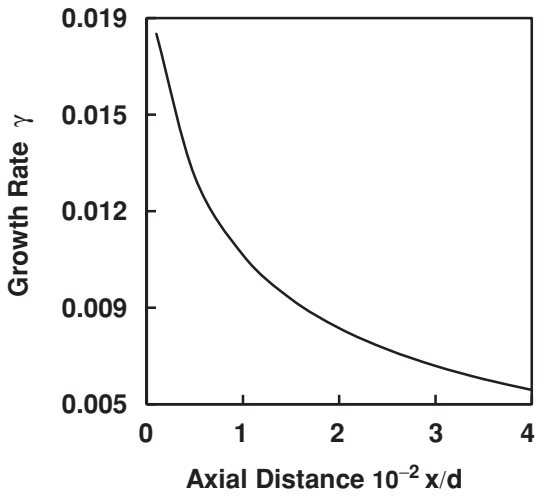

FIG. 11. Variation growth rate γ along the axial distance from the anode for the parameter as in Fig. 1.

Eq. (23), where the coefficients a_2 and a_3 show a dependence on the temperatures (T_i and T_e) and the electron gyrofrequency via terms $\frac{Y_i T_i k_y^2}{M}$, $\frac{2m\Omega^2 Y_i T_i}{Y_e T_e M}$, and $\frac{2k_y Y_i T_i u_0 \Omega^2 m}{M Y_e T_e}$. Physically it means the effect of gyratory motion of the electrons becomes less significant in the presence of higher electron temperature (T_e being in the denominator) when the other parameters are kept fixed. In contrast the ion temperature has the opposite effect with T_i being in the numerator. It can be seen that for higher electron temperature the coefficients a_2 and a_3 decrease which causes the coefficient m_1 to increase. This finally leads to the lower values of the oscillation frequency ω_3 and hence the smaller growth rate. On the other hand, the coefficients a_2 and a_3 attain higher values due to the coefficient m_1 being lowered, resulting in larger oscillation frequency ω_3 and the enhanced growth rate for the higher ion temperature. The enhanced perturbed potential ϕ with the ion and electron temperatures is shown in Figs. 9 and 10, respectively. The increased potential for the higher temperature of the plasma species is in agreement with an experiment [27].

Finally, in Fig. 11 we show the variation of growth rate with respect to axial distance from the anode. Evidently the instability grows at a smaller rate when we move away from the anode. It means the oscillations are more unstable in the region toward the anode. This can be understood based on the mobility of electrons and their residence time in the channel. According to Bohm's classical model the electron mobility increases along the axial distance from the anode. It means the residence time of the electrons is decreased in the ionization channel. This results in a reduction in the growth of the instability.

IV. CONCLUSIONS

We have analytically studied the growth rate of Rayleigh instability in a Hall thruster under the effect of finite ion and electron temperatures that were omitted in earlier investigations. Unlike other investigators, we obtain two interesting conditions (24) and (28) of the instability for the present plasma model. The oscillations whose frequency falls within the frequency band described by Eq. (28) are found to grow into instability, and the broader frequency band is observed for the real plasma when its species carry finite temperatures. It was found that higher frequency oscillations grow into instability if the plasma contains higher density gradient, the electrons drift with higher velocity, or stronger magnetic field is applied. Moreover, oscillations of larger wavelengths are found to be unstable even at lower frequency. The growth rate of the instability and the corresponding perturbed potential were observed to behave consistently.

ACKNOWLEDGMENTS

One of the authors (SS) would like to thank Council of Scientific and Industrial Research (CSIR), Government of India for providing financial support.

[1] V. V. Zhurin, H. R. Kaufman, and R. S. Robinson, Plasma Sources Sci. Technol. **8**, R-1 (1999).
[2] A. Bouchoule, J. P. Boeuf, A. Heron, and O. Duchemin, Plasma Phys. Control. Fusion **46**, B407 (2004).
[3] J. C. Adam, J. P. Boeuf, N. Dubuit, M. Dudeck, L. Garrigues, D. Gresillon, A. Heron, G. J. M. Hagelaar, V. Kulaev, N. Lemoine, S. Mazouffre, J. Perez Luna, V. Pisarev, and S. Tsikata, Plasma Phys. Controlled Fusion **50**, 124041 (2008).
[4] A. Bouchoule, Ch. Philippe-Kadlec, M. Prioul, F. Darnon, M. Lyszyk, L. Magne, D. Pagnon, S. Roche, M. Touzeau, S. Béchu, P. Lasgorceix, N. Sadeghi, N. Dorval, J.-P. Marque, and J. Bonnet, Plasma Sources Sci. Technol. **10**, 364 (2001).
[5] D. P. Schmidt, N. B. Meezan, W. A. Hargus Jr., and M. A. Cappelli, Plasma Sources Sci. Technol. **9**, 68 (2000).
[6] E. Y. Choueiri, Phys. Plasmas **8**, 1411 (2001).

[7] S. Chable and F. Rogier, Phys. Plasmas **12**, 033504 (2005).
[8] S. Barral and Z. Peradzynski, Phys. Plasmas **17**, 014505 (2010).
[9] M. Keidar, J. Appl. Phys. **103**, 053309 (2008).
[10] N. B. Meezan, W. A. Hargus Jr., and M.A. Cappelli, Phys. Rev. E **63**, 026410 (2001).
[11] C. A. Thomas, N. Gascon, and M. A. Cappelli, Phys. Rev. E **74**, 056402 (2006).
[12] A. A. Litvak, Y. Raitses, and N. J. Fisch, Phys. Plasmas **11**, 1701 (2004).
[13] A. Lazurenko, V. Krasnoselskikh, and A. Bouchoule, IEEE Trans. Plasma Sci. **36**, 1977 (2008).
[14] A. A. Litvak and N. J. Fisch, Phys. Plasmas **11**, 1379 (2004).
[15] A. Ducrocq, J. C. Adam, A. Héron, and G. Laval, Phys. Plasmas **13**, 102111 (2006).
[16] S. Barral and E. Ahedo, Phys. Rev. E **79**, 046401 (2009).
[17] F. Battista, E. A. De Marco, T. Misuri, and M. Andrenucci, *30th International Electric Propulsion Conference, Florence, Italy* (2007), p. 1.
[18] K. Komurasaki and Y. Arakawa, Acta Astronaut. **38**, 185 (1996).
[19] L. D. Landau and E. M. Lifshitz, *Fluid Mechanics* (Addison-Wesley, New York, 1959).
[20] E. Chesta, N. B. Meezan, and M. A. Cappelli, J. Appl. Phys. **89**, 3099 (2001).
[21] G. J. M. Hagelaar, J. Bareilles, L. Garrigues, and J. P. Boeuf, J. Appl. Phys. **93**, 67 (2003).
[22] A. Smirnov, Y. Raitses, and N. J. Fisch, J. Appl. Phys. **92**, 5673 (2002).
[23] L. Wei, B. Jiang, C. Wang, Hong Li, and D. Yul, Plasma Sources Sci. Technol. **18**, 045020 (2009).
[24] M. Keidar and I. D. Boyd, J. Appl. Phys. **86**, 4786 (1999).
[25] Y. V. Esipchuck and G. N. Tilinin, Sov. Phys. Tech. Phys. **21**, 417 (1976).
[26] L. B. King, A. D. Gallimore, and C. M. Marrese, J. Propul. Power **14**, 327 (1998).
[27] D. Kusamoto, K. Mikami, K. Komurasaki, and A. D. Gallimore, Trans. Jpn. Soc. Aeronaut. Space Sci. **40**, 238 (1998).